tive in reducing the oscillation amplitudes and the corresponding results are represented by the circles in Fig. 4.

The inverted wing with the planar upper surface presents a case where the flaps' leading edge is closer to the vortices originating from the leading-edge portion ahead of the flaps. Consequently, for this configuration, smaller oscillation amplitudes are expected (indeed, as shown by the diamond symbols in Fig. 4) due to the larger effect of the flap motion.

Acknowledgment

This work was supported by NASA Ames Research Center, under Grant NCC-2-458, with James Ross as project monitor.

References

[1]Nguyen, L. T., Yip, L., and Chambers, J. R., "Self Induced Wing Rock of Slender Delta Wings," AIAA Paper 81-1883, Aug. 1981.

[2]Levin, D., and Katz, J., "Dynamic Load Measurements with Delta Wings Undergoing Self-Induced Roll Oscillations," *Journal of Aircraft*, Vol. 21, Jan. 1984, pp. 30–36.

[3]Katz, J., and Levin, D., "Self-Induced Roll-Oscillations Measured on a Delta Wing/Canard Configuration," *Journal of Aircraft*, Vol. 23, Nov. 1986, pp. 801–807.

[4]Jun, Y. W., and Nelson, R. C., "Leading Edge Vortex Dynamics on a Slender Oscillating Wing," *Journal of Aircraft*, Vol. 25, Sept. 1988, pp. 815–819.

[5]Ng, T. T., Malcolm, G. N., and Lewis, L. C., "Flow Visualization Study of Delta Wing in Wing-Rock Motion," AIAA Paper 89-2187, Aug. 1989.

[6]Arena, A. S., and Nelson, R. C., "The Effect of Asymmetric Vortex Wake Characteristics on a Slender Delta Wing Undergoing Wing Rock Motion," AIAA Paper 89-3348, Aug. 1989.

[7]Levin, D., and Katz, J., "Self-Induced Roll Oscillations of Low-Aspect Ratio Rectangular Wings," AIAA Paper 90-2811, Aug. 1990.

[8]Arena, A. S., and Nelson, R. C., "Unsteady Surface Pressure Measurements on a Slender Delta Wing Undergoing Limit Cycle Wing Rock," AIAA Paper 91-0434, Jan. 1991.

[9]Konstadinopoulos, P., Mook, D. T., and Nayfeh, A. H., "Numerical Simulation of the Subsonic Wing Rock Phenomenon," AIAA Paper 83-2115, Aug. 1983.

[10]Ericsson, L. E., "The Fluid Mechanics of Slender Wing Rock," *Journal of Aircraft*, Vol. 21, May 1984, pp. 322–328.

[11]Konstadinopoulos, P., Mook, D. T., and Nayfeh, A. H., "Subsonic Wing Rock of Slender Delta Wings," *Journal of Aircraft*, Vol. 22, No. 3, 1985, pp. 223–228.

[12]Ericsson, L. E., "Analytic Prediction of the Maximum Amplitude of Slender Wing Rock," *Journal of Aircraft*, Vol. 26, No. 1, 1989, pp. 35–39.

[13]Hsu, C. H., and Lan, C. E., "Theory of Wing Rock," *Journal of Aircraft*, Vol. 22, No. 10, 1985, pp. 920–924.

[14]Elzebda, J. M., Mook, D. T., and Nayfeh, A. H., "Influence of Pitching Motion on Subsonic Wing Rock of Slender Delta Wings," *Journal of Aircraft*, Vol. 26, No. 6, 1989, pp. 503–508.

[15]Elzebda, J. M., Nayfeh, A. H., and Mook, D. T., "Development of an Analytical Model of Wing Rock for Slender Delta Wings," *Journal of Aircraft*, Vol. 26, No. 8, 1989, pp. 737–743.

[16]Lee, E. M., and Batina, J. T., "Conical Euler Simulation of Wing Rock for a Delta Wing Planform," *Journal of Aircraft*, Vol. 28, No. 1, 1991, pp. 94–96.

[17]Ericsson, L. E., "Slender Wing Rock Revisited," AIAA Paper 91-0417, Jan. 1991.

[18]Malcolm, G. N., Ng, T. T., Lewis, L., and Murri, D. G., "Development of Non-Conventional Control Methods for High Angle of Attack Flight Using Vortex Manipulation," AIAA Paper 89-2192, July 1989.

[19]Rao, D. M., and Puram, C. K., "Chine Forebody Vortex Manipulation by Mechanical and Pneumatic Techniques on a Delta Wing Configuration," AIAA Paper 91-1812, June 1991.

[20]Ng, T., Ong, L., Suarez, C., and Malcolm, G., "Wing Rock Suppression Using Forebody Vortex Control," AIAA Paper 91-3227, Sept. 1991.

[21]Luo, J., and Lan, E., "Control of Wing-Rock Motion of Slender Delta Wings," AIAA Paper 91-2886, Aug. 1991.

[22]Verhaagen, N. G., "An Experimental Investigation of the Vortex Flow over Delta and Double-Delta Wings at Low Speed," Aerodynamics of Vortical Type Flows in Three Dimensions, AGARD CP-342, Paper 7, Rotterdam, The Netherlands, April 1983.

[23]Erickson, G. E., "Water Tunnel Flow Visualization: Insight into Complex Three-Dimensional Flowfields," *Journal of Aircraft*, Vol. 17, No. 9, 1980, pp. 656–662.

[24]Hoejimakers, H. W. M., Vaatsra, W., and Verhaagen, N. G., "Vortex Flow over Delta and Double-Delta Wings," *Journal of Aircraft*, Vol. 20, No. 9, 1983, pp. 825–832.

[25]Rae, W. H., Jr., and Pope, A., "Low-Speed Wind Tunnel Testing," Wiley, New York, 1984, p. 371.

[26]Morris, S. L., and Ward, D. T., "A Video-Based Experimental Investigation of Wing Rock," AIAA Paper 89-3349, Boston, MA, Aug. 1989.

[27]Walton, J., and Katz, J., "Reduction of Wing Rock Amplitudes Using Leading-Edge Vortex Manipulations," AIAA Paper 92-0279, Reno, NV, Jan. 1992.

Effects of Wing-Tip Vortex Flaps

Lance W. Traub* and Alan Nurick†
University of the Witwatersrand, Johannesburg, South Africa

Nomenclature

AR	=	aspect ratio, b^2/S
b	=	wing span
C_D	=	drag coefficient, drag/qS
C_L	=	lift coefficient, lift/qS
C_{L_α}	=	lift curve slope
C_M	=	pitching moment coefficient, moment/qSc
c	=	reference chord
e	=	Oswald efficiency factor
q	=	dynamic pressure of freestream
S	=	projected planform area
α	=	angle of attack
δ_F	=	wing tip vortex flap angle

Subscripts

cdmin	=	lift coefficient at which minimum drag occurs
min	=	minimum drag coefficient
0	=	zero lift

Introduction

THE trailing vortex system of a finite lifting wing induces a downwash, and as a consequence a rotation of the freestream velocity vector giving rise to vortex drag.

The importance of wing tip geometry in the generation of vortex drag has propagated several tip-mounted drag reducing devices aimed at improving wing efficiency. Successful concepts include winglets[1–3] and tip sails.[4,5]

Recently, the planar sheared tip has received attention, and its most extreme application (the planar crescent wing) is attributed with a theoretical efficiency exceeding that of a wing with elliptic loading.[6] Vijgen et al.[7] reported in an investigation of sheared tip aerodynamics, an increase in both $(L/D)_{max}$ and aerodynamic efficiency for sheared wings over a comparative basic wing. Naik et al.[8] in comparing a high-aspect ratio wing with a rectangular, elliptic, and a sheared tip, reported the lowest Oswald efficiency factor for the sheared tip. These contradictory results suggest that the performance of sheared tips has not been fully characterized. The drag

Received July 13, 1992; revision received Sept. 15, 1992; accepted for publication Sept. 15, 1992.

*Graduate Student, 1 Jan Smuts Ave., P.O. Wits, 2050.

†Professor, Branch of Aeronautical Engineering, 1 Jan Smuts Ave., P.O. Wits, 2050.

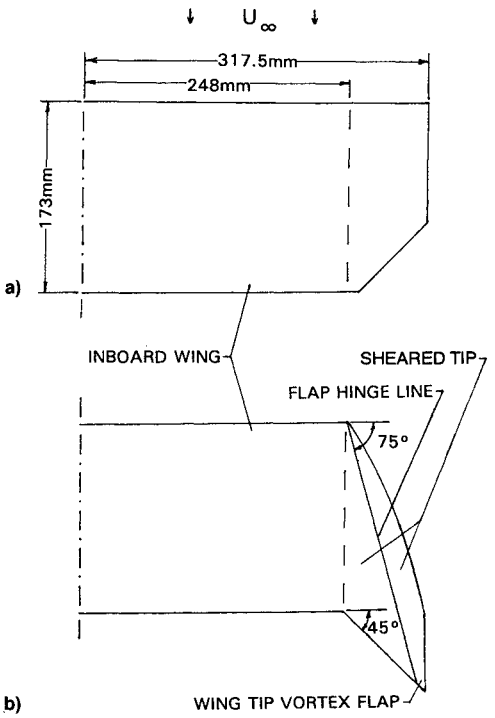

Fig. 1 Geometry of the tip configurations tested: a) basic wing and b) sheared wing showing wing tip vortex flap geometry.

reductions ascribed to sheared tips may be attributed to wake deformation effects and changes in spanwise load distribution.[7]

An experimental investigation of sheared tips modified to form a wing tip vortex flap (WTVF) as shown in Fig. 1b is presented. The effect of similar devices has been determined on slender delta wings.[9-11] On these wings the flap is formed by rotating a full span leading-edge extension either above or below the plane of the wing. This has the effect of concentrating the suction of the leading edge vortex on the flap.[10] When the flap is appropriately deflected a component of the induced vortex force can oppose drag. In a similar manner, it is suggested that a flap placed on the wing tip (Fig. 1b), and appropriately deflected, may reduce drag by utilizing the suction of the tip vortex if the vortex is "captured" by the flap.

Experimental Equipment and Procedure

A wind-tunnel investigation was conducted in the University of the Witwatersrand's low-speed continuous wind tunnel. This tunnel has an elliptic cross section with a minor axis of 610 mm and a major axis of 910 mm. The geometry of the tip configurations tested is shown in Fig. 1. Applicable dimensions and aspect ratios are given in Table 1. The basic wing shown in Fig. 1a consisted of a tip extension attached to a rectangular flat plate wing. The wing had a rounded leading edge, and a beveled trailing edge. For the aspect ratio of this tip form to be comparable with those of the sheared configurations, the outer rear trailing edges of the basic wing were removed. The sheared tip extensions were attached to the same inboard wing, and had a gothic planform as shown in Fig. 1b. The hinge-line sweep angle was 75 deg, and the trailing edge sweep angle was 45 deg. The sheared tip profile was then rotated about its flap "hinge-line" to form a WTVF. The flap angle δ_F was measured perpendicular to the flap hinge-line. A positive flap angle was defined as one where the flap was rotated below the plane of the wing. The leading edge of the WTVF was sharp to enforce flow separation.

A six-component Pyrimidal balance was used to determine the forces and moments acting on the wing. By repeating tests for a given configuration the repeatability of the balance was estimated as:

$$C_L = \pm 0.0014$$

$$C_D = \pm 0.0008$$

$$C_M = \pm 0.0039$$

Table 1 Dimensions and aspect ratios of tested models

δ_F	S, m^2	b, m	AR
−30 deg	0.1046	0.631	3.81
0 deg	0.1057	0.638	3.85
15 deg	0.1054	0.634	3.81
20 deg	0.1052	0.633	3.81
25 deg	0.1049	0.632	3.81
30 deg	0.1046	0.631	3.81
Basic wing	0.1049	0.635	3.84

All the forces and moments from the tests were corrected for blockage using the procedure outlined in Ref. 12. Tare and interference effects as well as the tunnel flow angularity were established using an image system.[12] Tests were conducted at a freestream velocity of ≈46 m/s (equivalent to a Mach number of ≈0.13), corresponding to a dynamic pressure head of approximately 1050 Pa. The set angle of attack was varied from −2 to 22 deg in 2 deg increments. The Reynolds number was 430,000, based on a root chord length of 173 mm.

All forces and moments were nondimensionalized using the projected planform area of the respective configuration. All moments were referred to the wing's quarter chord. In the tests the WTVF angle was varied.

Results

The WTVF of the sheared tip shown in Fig. 1b was positioned at $\delta_F = -30$, 0, 15, 20, 25, and 30 deg. A summary of results for these configurations is given in Table 2. The results obtained using some of these flap angles are omitted in the graphical presentation of the data to improve clarity. Figure 2 shows the lift curves for the above. From the data it appears that deflecting the tip flap has a similar (but opposite) effect to that of deflecting a trailing-edge flap, in that α_0 shifts negative for the negative flap angle, and positive flap angles move α_0 positive. There is a gradual reduction in the lift curve slope and lift value with downward flap deflection, as shown in Fig. 2 and Table 2. $C_{L_{max}}$ also reduces as the flap is deflected downwards. It is probable that the lift increments are due to increased vortex lift generation, and increased potential lift from the tip regions (on surface flow visualization verified that flow separation adjacent to the tip was reduced, however, space limitations do not allow inclusion of this data). This is especially so for $\delta_F = -30$ deg as the wing tips are at a greater effective incidence than the rest of the wing due to their upward cant. The nature of the stall is gradual for all angles, with a peak being less pronounced with downward flap rotation. Up to $C_L \approx 0.55$, the sheared tip with $\delta_F = 0$ deg and basic wing have similar performance. At higher angles of attack in the nonlinear range, the lift of the basic wing drops off more than most of the WTVF configurations, and approaches that with $\delta_F = 25$ deg.

The drag polar for the various WTVF angles is shown in Fig. 3. In the low-to-moderate lift regions ($C_L < 0.5$) there is minimal variation in drag between the various flap settings. This may be attributed to the fact that all the configurations have equal wetted areas. For a C_L greater than 0.6, drag reduces with upward flap deflection. This may be ascribed to the reduction in required angle of attack for a given lift coef-

Table 2 Data summary for tested configurations

δ_F	α_0	C_{L_α}, deg^{-1}	$C_{L_{max}}$	e
−30 deg	−0.27 deg	0.070	0.802	0.325
0 deg	0 deg	0.068	0.778	0.321
15 deg	0.17 deg	0.067	0.765	0.338
20 deg	0.24 deg	0.067	0.762	0.330
25 deg	0.30 deg	0.066	0.753	0.327
30 deg	0.36 deg	0.065	0.751	0.322
Basic wing	0 deg	0.069	0.749	0.320

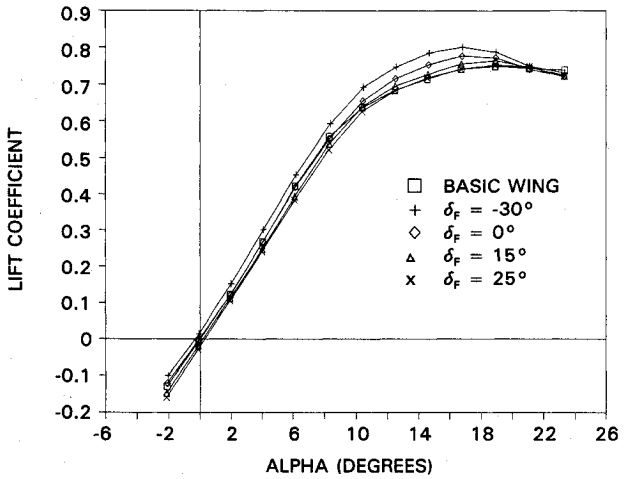

Fig. 2 Effect of WTVF deflection angle on measured lift coefficient.

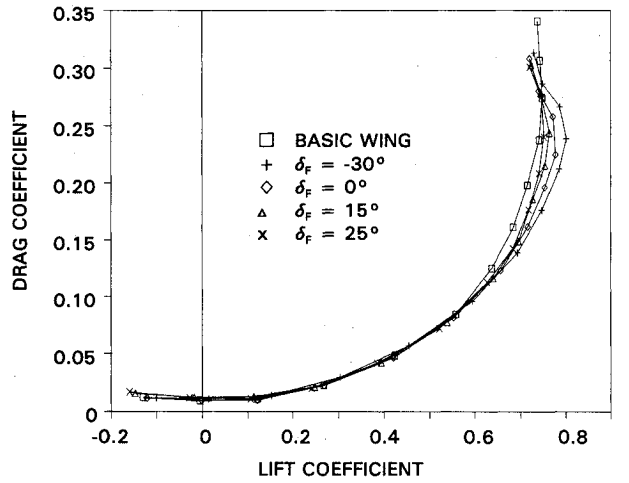

Fig. 3 Effect of WTVF deflection angle on measured drag polar.

ficient. At a lift coefficient of 0.7, the drag reduction compared to the basic wing is 20.1 and 16.5% for $\delta_F = -30$ and 0 deg, respectively. In Fig. 2 it may be seen that at high angles of attack the lift coefficient of the sheared tip wing with a WTVF angle of 25 deg is the same as that of the basic wing and yet, as shown in Fig. 3, experiences a large reduction in drag. This could be attributed to a component of thrust being generated by the vortex flaps.

As the effect of WTVF deflection is analogous to that of camber, it would be reasonable to approximate drag as

$$C_D = C_{D_{min}} + (C_L - C_{L_{cdmin}})^2/(\pi ARe) \qquad (1)$$

The Oswald efficiency factors in Table 2 were calculated using Eq. (1). Unfortunately the constant e incorporates vortex and pressure drag, both of which vary with the square of the lift coefficient. To separate out the two components is difficult, thus the tabulated e values include viscous effects. It can be seen in Table 2 that induced performance (e) in the linear lift range is roughly similar for most of the flap angles, with the sheared tip with $\delta_F = 15$ deg recording the highest efficiency factor, an increase of 5.6% over the basic wing.

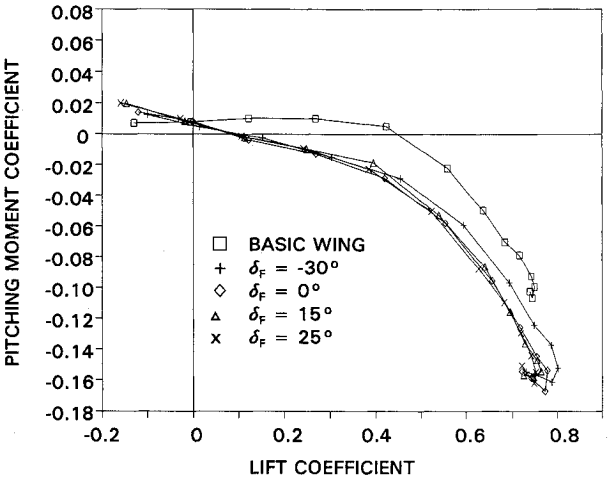

Fig. 4 Effect of WTVF deflection angle on measured pitching moment.

Figure 4 shows pitching moment as a function of lift coefficient. It is apparent that the addition of the sheared tips leads to an increase in nose down pitching moment. The action of the tip vortices would probably lead to reduced flow separation in the tip regions.[7] The basic wing has an approximately constant value of dC_M/dC_L up to a lift coefficient of 0.4. This indicates that the aerodynamic center of the flat plate wing was located approximately at the reference point where the measurements were made, i.e., at the quarter chord.

Conclusions

From the experimental data the following conclusions may be drawn:

In the nonlinear lift range at lift coefficients greater than 0.6, all the sheared wing WTVF angles showed a drag reduction compared to the basic wing. This reduction increased as the WTVF was rotated upwards and was a maximum for $\delta_F = -30$ deg. Similarly $C_{L_{max}}$ increased as the WTVF was rotated upwards, and was also a maximum for $\delta_F = -30$ deg. In the linear lift range, $\delta_F = 15$ deg recorded the best induced efficiency. Varying the wing tip vortex flap angle had a similar, but opposite, effect to that of camber addition, with α_0 shifting negative for a negative flap angle and vice versa. The addition of the sheared tips increased nose down pitching moment.

Due to the low Reynolds number at which the tests were conducted, the validity of the results at higher Reynolds number is uncertain, as is their relevance to higher aspect ratios.

References

[1]van Dam, C. P., Holmes, B. J., and Pitts, C., "Effect of Winglets on Performance and Handling Qualities of General Aviation Aircraft," *Journal of Aircraft*, Vol. 18, No. 7, 1981, pp. 587–591.

[2]Heyson, H. H., Riebe, G. D., and Fulton, C. L., "Theoretical Parametric Study of the Relative Advantages of Winglets and Wing-Tip Extensions," NASA TP 1020, Sept. 1977.

[3]Asai, K., "Theoretical Considerations in the Aerodynamic Effectiveness of Winglets," *Journal of Aircraft*, Vol. 22, No. 7, 1985, pp. 635–637.

[4]Spillman, J. J., "The Use of Wing Tip Sails to Reduce Vortex Drag," *Aeronautical Journal*, Sept. 1978, pp. 387–395.

[5]Spillman, J. J., "Wing Tip Sails; Progress to Date and Future Developments," *Aeronautical Journal*, Dec. 1987, pp. 445–453.

[6]van Dam, C. P., "Induced-Drag Characteristics of Crescent-Moon-Shaped Wings," *Journal of Aircraft*, Vol. 24, No. 2, 1987, pp. 115–119.

[7]Vijgen P. M. H. W., Van Dam, C. P., and Holmes, B. J., "Sheared Wing Tip Aerodynamics: Wind-Tunnel and Computational Investigation," *Journal of Aircraft*, Vol. 26, No. 3, 1989, pp. 207–213.

[8]Naik, D. A., and Ostowari, C., "Effects of Nonplanar Outboard Wing Forms on a Wing," *Journal of Aircraft*, Vol. 27, No. 2, 1990, pp. 117–122.

[9]Grantz, A. C., and Marchmann, J. F., "Trailing Edge Flap Influence on Leading Vortex Flap Aerodynamics," *Journal of Aircraft*, Vol. 20, No. 2, 1983, pp. 165–169.

[10]Rao, D. M., "An Exploratory Study of Area-Efficient Vortex Flap Concepts," *Journal of Aircraft*, Vol. 20, No. 12, 1983, pp. 1062–1067.

[11]Marchmann, J. F., "The Aerodynamics of Inverted Leading Edge Vortex Flaps on Delta Wings," AIAA Paper 81-0356, Jan. 1981.

[12]Pope, A., and Rae, W.H., "Low-Speed Wind Tunnel Testing," Wiley, New York, 1984, pp. 199–208, 362–424.